Journal of Alloys and Compounds 931 (2023) 167559

Contents lists available at ScienceDirect

Journal of Alloys and Compounds

journal homepage: www.elsevier.com/locate/jalcom

All-d-metal Ni(Co)-Mn(X)-Ti (X = Fe or Cr) Heusler alloys: Enhanced magnetocaloric effect for moderate magnetic fields

Aun N. Khan, Luis M. Moreno-Ramírez *, Álvaro Díaz-García, Jia Yan Law, Victorino Franco *

Dpto. Física de la Materia Condensada, ICMS-CSIC, Universidad de Sevilla, P.O. Box 1065, Sevilla 41080, Spain

ARTICLE INFO

Article history:
Received 29 July 2022
Received in revised form 28 September 2022
Accepted 10 October 2022
Available online 12 October 2022

Keywords:
All-d-metal Heusler alloys
Ni(Co)-Mn-Ti
Magnetostructural transition
Magnetocaloric effect

ABSTRACT

All-d-metal Ni(Co)-Mn-Ti Heusler alloys show high magnetocaloric/barocaloric effects ascribed to the occurrence of a martensitic transformation together with excellent mechanical properties. However, high magnetic fields are needed to fully drive the transformation and to obtain their maximum responses. To further tune the martensitic transition and the associated magnetocaloric response, we systematically investigate the role of partial Mn substitution by Fe or Cr on the parent composition $Ni_{36}Co_{14}Mn_{35}Ti_{15}$. On the one hand, Cr doping increases the entropy change of the transformation but causes a tighter overlap of both martensitic and Curie transitions. This significantly reduces the magnetization difference between austenite and martensite and, consequently, strongly decreases the magnetocaloric response. On the other hand, Fe doping reduces the entropy change of the transformation and separates both martensitic and Curie transitions while keeping the magnetization difference among both phases. These two combined features reduce the magnetic field needed to completely drive the martensitic transformation and leads to higher and broader isothermal entropy change peaks for moderate magnetic field changes, reaching up to 25% enhancement for 2 T when compared to the undoped alloy.

1. Introduction

Materials exhibiting magnetocaloric (MC) effect are still increasingly getting scientific attention due to their application in solid-state magnetic refrigeration devices [1,2]. These devices are called to replace conventional gas compression-expansion refrigeration systems due to their larger energy efficiency and the avoidance of harmful substances [3,4]. Moreover, these MC refrigeration systems are expected to be used not only for room temperature applications but also in other high-demand applications at cryogenic temperatures related to the liquefaction of hydrogen as an energy vector [5]. The MC effect is quantified by the temperature change produced in adiabatic conditions or by the entropy change produced in isothermal conditions during magnetic field application/removal. Both magnitudes are maximal in the vicinity of a thermomagnetic phase transition and, therefore, MC materials are classified according to the order of the phase transition that they undergo, either first- (FOPT) or second-order (SOPT) type [6]. Typically, materials undergoing FOPT show significantly larger MC responses than those undergoing SOPT and, therefore, since the discovery of a so-called giant effect in $Gd_5(Si,Ge)_4$ alloys [7], most studied materials nowadays belong to the FOPT category [8]. Some well-known families of FOPT MC materials are $La(Fe,Si)_{13}$ [9,10], $(Mn,Fe)_2(P,Si)$ [11] and Heusler alloys [12,13].

Heusler alloys are an interesting and versatile class of ternary intermetallic alloys with XYZ or X_2YZ stoichiometry (half or full Heusler, respectively), although they can be also off-stoichiometric. Typically, X and Y are transition metal elements and Z is an element of III-VA group of the periodic table [14]. Among the various FOPT Heusler alloys, Ni-Mn-Z (Z = In, Sn or Ga) alloys are intensively studied because of their multifunctional properties including magnetocaloric effect [15–17]. However, their intrinsic brittleness, usual in intermetallic compounds, together with the volume changes during the transformation lead to mechanical instabilities which degrade the response under cyclic working conditions [18,19]. Improved mechanical performance has been found in all-d-metal Heusler alloys which is attributed to strong interatomic bonding force of the d-d orbital with respect to the covalent character of the p-d orbital hybridization [20,21]. Recently, a novel all-d-metal Ni-Co-Mn-Ti composition was proposed by Wei et al. showing enhanced mechanical properties when compared to the previous Ni-Mn-Ti alloys [22]. In this system, off-stoichiometry compositions lead to a magnetostructural transition and the stabilization of the austenitic phase

* Corresponding authors.
E-mail addresses: lmoreno6@us.es (L.M. Moreno-Ramírez), vfranco@us.es (V. Franco).

https://doi.org/10.1016/j.jallcom.2022.167559
0925-8388/

[20]. With respect to their magnetic behavior, Ni substitution by Co is necessary for having a large magnetization change between martensitic and austenitic phases [23–25]. These improved mechanical and magnetic properties would lead to better durability and to the extension of the material into a multicaloric stimuli devices (e.g., combining magneto- and baro-caloric effects) [24]. The stoichiometric variation or partial atomic substitutions would lead to changes in the electron interaction, a unique feature which is expressed as the valence electron concentration per atom (e/a) ratio [21]. However, further optimization is still needed: the obtained response requires high magnetic field changes to reach saturation (to complete the transformation from austenite to martensite and vice-versa) and there exist significant thermal and magnetic hysteresis associated to the response which are detrimental for MC applications [26].

Compositional modification via element substitution is the most employed and easier strategy for tunning the magnetocaloric response in bulk materials. In this work, the influence on the martensitic transition and magnetocaloric effect of partial substituting Mn by Fe or Cr in the reference composition $Ni_{36}Co_{14}Mn_{35}Ti_{15}$ are studied. On the one hand, Mn atoms have been selected because, despite their complex magnetic behavior making them a promising target for substitutions, most of the substitutions presented in the literature focus on Ni [27,28]. On the other hand, Fe and Cr have been selected for having similar atomic radius but different number of valence electrons and magnetic moment. It is found that while Cr doping has a clear detrimental effect on magnetic behavior of the martensitic transformation and, therefore, on the magnetocaloric effect, Fe doping leads to a significantly enhanced magnetocaloric effect at the desired field range of 2 T. This improvement for Fe doping is associated to the separation of the martensitic and Curie transitions together with a significant decrease of the entropy change of the transformation [29,30]. Moreover, both features allow to reduce the magnetic field needed to induce the transformation from paramagnetic martensite to ferromagnetic austenite, increasing the shifting of the martensitic transition with field and the width of the MC response.

2. Materials and methods

Starting from $Ni_{36}Co_{14}Mn_{35}Ti_{15}$ as reference composition, two alloy series partially substituting Mn by Fe or Cr were produced with nominal compositions of $Ni_{36}Co_{14}Mn_{35-x}Fe_xTi_{15}$ (where x = 3, 5 and 7) and $Ni_{36}Co_{14}Mn_{35-y}Cr_yTi_{15}$ (where y = 1 and 3). The different samples were produced by arc melting (Edmund Bühler MAM-1) starting from raw materials (at least 99.9% purity) in argon-controlled atmosphere. The resulting ingots were melted and flipped four times to ensure homogeneity. An extra 6 wt% of Mn was added to compensate the evaporation losses during arc-melting. The as-cast ingots were annealed at 1273 K for 4 days and then quenched in water. Samples are denoted by the nominal doping content of the alloys as Fe3, Fe5, Fe7, Cr1 and Cr3, whereas the reference alloy is designated as Ref.

Microstructure and composition were characterized using powder X-ray diffraction (XRD, Bruker D8I diffractometer with Cu-Kα radiation) and scanning electron microscopy equipped with energy dispersive X-ray spectrometry (SEM-EDX; FEI™ Teneo). To evaluate compositional uniformity, at least three EDX point analyses were performed at different regions. The final compositions were obtained by taking an average of the different points, which showed no significant deviations among them. Thermal analysis was carried out using a TA Instruments Q20 differential scanning calorimeter (DSC) at a heating rate of 10 K/min. Temperature dependence of magnetization measurements were performed in a Lake Shore 7407 vibrating sample magnetometer (VSM). For minimizing the demagnetizing factor, samples were selected with plate-like shapes (approximately 2 ×1 ×0.1 mm) and a mass of 3 mg, with the magnetic field applied in-plane along the length of the plate. In addition, three different pieces from the annealed ingot were $M(T)$ tested, showing good reproducibility of the results. Curie temperatures, T_C, and martensitic transition temperatures, T_{trans}, were determined from the inflection points of magnetization vs. temperature at 5 mT. Magnetic field dependence of magnetization measurements up to 9 T were performed in the VSM option of a Quantum Design Physical Property Measurement System (PPMS). The isothermal entropy change, ΔS_{iso}, was indirectly obtained from isothermal magnetization measurements using a discrete approximation to the following equation [1,31]:

$$\Delta S_{iso} = \mu_0 \int_0^H \left(\frac{\partial M}{\partial T}\right)_{H'} dH', \tag{1}$$

where μ_0 is the magnetic permeability of vacuum, M the magnetization, T the temperature and H the magnetic field. Due to the significant magnetic hysteresis of the studied alloys, discontinuous protocols for erasing the history of the samples prior to any isothermal magnetization measurement were performed [6,32,33]. From ΔS_{iso} data, the field dependence exponent n was calculated using the following equation [34]:

$$n = \frac{d\ln|\Delta S_{iso}|}{d\ln H} \tag{2}$$

To evaluate the magnetocaloric performance and to compare it with literature data, the temperature averaged entropy change over a span of 5 K, $TEC(5)$, was calculated. For its calculation, the following approximation was made [35]:

$$TEC(5) \approx \frac{\Delta S_{iso}(T_{pk} - 2.5\ \mathrm{K}) + \Delta S_{iso}(T_{pk}) + \Delta S_{iso}(T_{pk} + 2.5\ \mathrm{K})}{3}, \tag{3}$$

where T_{pk} is the temperature corresponding to the peak value of ΔS_{iso}. This approach simplifies the calculation from literature data, avoiding the digitization of the whole curves [36,37].

3. Results and discussion

Fig. 1 shows the room temperature powder XRD spectra for the series. For Ref sample, a majority of the modulated 5M monoclinic martensite is observed (indexed by gray dashed lines) in addition to minority of B2 austenite (indexed by red dotted lines) and Ni_3Ti (approx. 4%). For Cr doped samples, 5M martensite becomes more prominent and only small amount of $L1_0$ phase (approx. 10%) is detected with higher Cr additions (Cr3). On the other hand, for Fe doped samples, in addition to the martensite, peaks corresponding to B2 austenite are also observed. With higher Fe additions (Fe5 and Fe7), weak peaks corresponding to the tetragonal $L1_0$ structure are observed (indexed by blue triangles), estimated to approx. 15 and 10 wt%. The phase identification from XRD analysis agree with previous works [20,22,38]. The obtained results indicate that Mn replacement by Fe stabilize the austenitic phase whereas Cr has an opposite effect as it stabilizes the martensitic phase.

Backscattered scanning electron (BSE) images of the different samples were taken on the polished surfaces at room temperature (Fig. 2). They reveal a relatively homogeneous composition for all samples, except for Fe5 and Fe7, in addition to the main phase whose composition corresponds to the nominal, a minor phase which could be the $L1_0$ structure identified in XRD is also observed. For Fe5, the

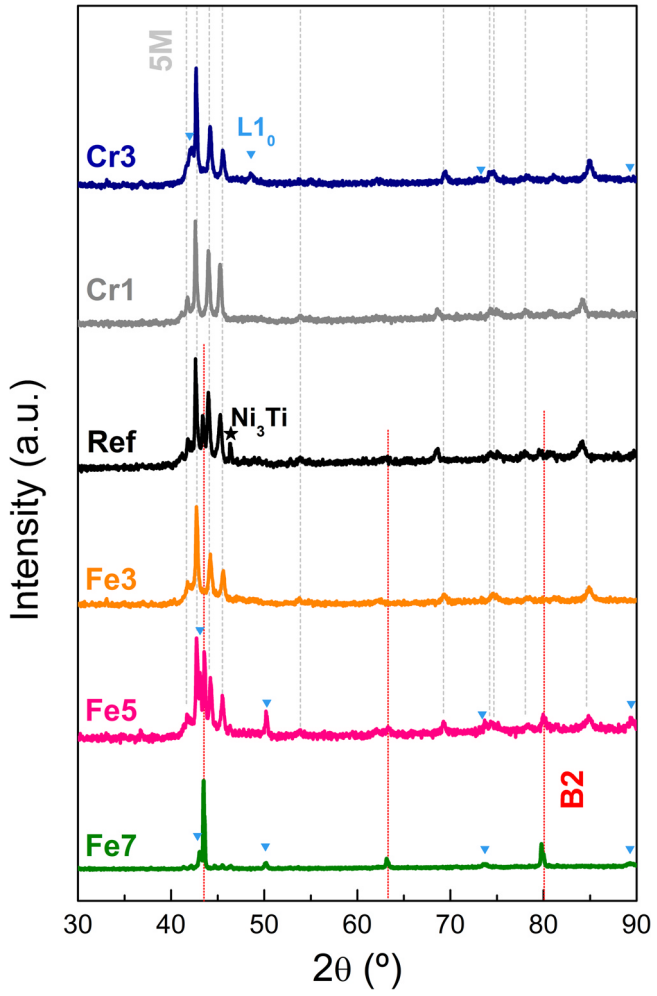

Fig. 1. Room temperature XRD spectra for the studied series. Indexed peaks for 5M, B2 and $L1_0$ structures.

secondary phase is enriched in Ni and Ti (labeled by A in Fig. 2) and for Fe7 it is depleted in Ti (labeled by B in Fig. 2). Compositions of these observed main and secondary phases are further summarized in Table 1. It is observed that the measured compositions of the samples are in good agreement with the nominal compositions. For Cr3 and Ref, although XRD spectra shows minor amounts of secondary phases, different contrast regions are not identified in the BSE images. This could happen to Heusler-type alloys as the sample pulverization step during XRD preparation can affect the phase transformation, differing from the bulk counterparts [39,40].

Fig. 3**a** illustrates the heating DSC scans for the studied series, where well-defined peaks are observed. With Cr additions, martensitic phase is stabilized whereas the Fe additions stabilizes austenitic phase, which also agree with the XRD observations. The transformation temperatures (Fig. 3**b**), obtained from the peak temperature of the DSC curves, decrease as the e/a ratio increases. The effect for Fe doping is − 10(1) K/at% while it is 28(2) K/at% for Cr doping, which is almost three times larger. The entropy change due to the transformation is calculated as $\Delta S_{\text{trans}} = \int \frac{dQ}{T}$ dT [41], with values depicted in Fig. 3**c**. There also exists a clear trend, with the transformation entropy change decreasing as the e/a ratio increases (in agreement with the temperature change trend, the transformation entropy change decreases with Fe and increases with Cr doping). It should be highlighted that the performed doping not only modifies the e/a ratio but also helps in obtaining different trends of the magnitudes for Fe and Cr doping.

Fig. 4**a** shows the temperature dependence of magnetization for the alloy series for an applied field of 5 mT. All the samples show a gradual increase of magnetization upon heating, which corresponds to the martensitic transition, followed by a decrease in magnetization due to the Curie transition of austenitic phase. When cooling, the martensitic transformation shifts to lower temperatures, which accounts for the characteristic hysteretic behavior of the transformation. It is also observed that the Curie transition of the austenitic phase slightly increases with Fe doping while it is significantly reduced by Cr doping (the Curie temperature of the austenite is marked by arrows). Fig. 4**b** shows the martensitic transition temperature values upon heating and cooling from magnetization measurements. This agrees with the trend observed previously from DSC measurements: the transition temperature decreases as the e/a ratio increases. These combined effects (shifts of the martensitic temperature and the Curie temperature upon doping) lead to the separation of the of martensitic and Curie transitions for Fe doping, while they become tightly overlapped for Cr doping. For Cr3, the magnetization values are zoomed 100 times, indicating the low magnetic response of both austenite and martensite. This is due to

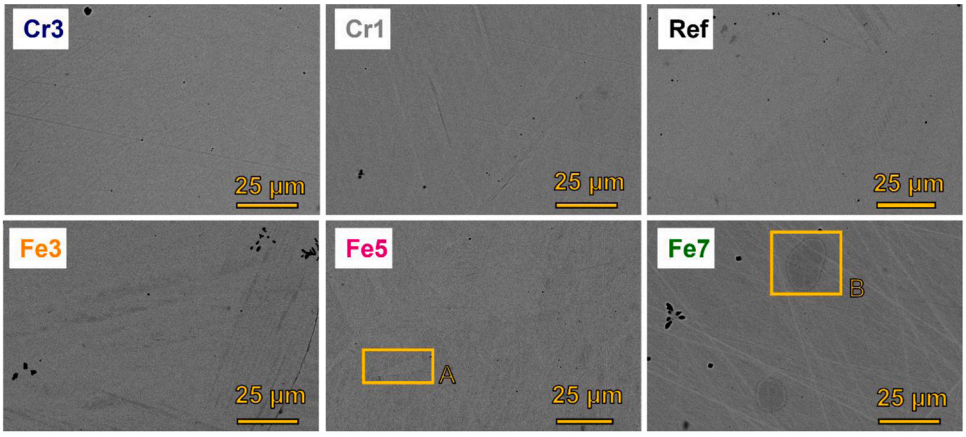

Fig. 2. BSE images of the studied series where A and B represent observed secondary phases.

Table 1
Compositions determined from EDX analysis. A and B indicate secondary phases found for Fe5 and Fe7, respectively.

Sample	Label	Nominal e/a ratio	Spot	Ni (at%)	Co (at%)	Mn (at%)	Doping element (at%)	Ti (at%)
$Ni_{36}Co_{14}Mn_{28}Fe_7Ti_{15}$	Fe7	7.98	Main phase	34.4(1.1)	13.9(1.3)	31.2(1.1)	4.8(1.5)	15.6(1.2)
			B	35.5(1.1)	13.4(1.3)	31.8(1.0)	9.6(1.2)	9.7(1.4)
$Ni_{36}Co_{14}Mn_{30}Fe_5Ti_{15}$	Fe5	7.96	Main phase	34.1(1.1)	14.0(1.3)	33.1(1.1)	3.7(1.7)	14.2(1.2)
			A	49.1(1.0)	14.6(1.1)	10.6(1.5)	3.0(2.1)	22.6(1.1)
$Ni_{36}Co_{14}Mn_{32}Fe_3Ti_{15}$	Fe3	7.94		34.6(1.1)	14.6(1.3)	33.9(1.1)	1.9(2.4)	15.0(1.2)
$Ni_{36}Co_{14}Mn_{35}Ti_{15}$	Ref	7.91		34.4(1.1)	14.7(1.3)	35.8(1.1)	–	15.2(1.2)
$Ni_{36}Co_{14}Mn_{34}Cr_1Ti_{15}$	Cr1	7.90		33.9(1.1)	14.8(1.3)	35.9(1.1)	1(4)	15.3(1.2)
$Ni_{36}Co_{14}Mn_{32}Cr_3Ti_{15}$	Cr3	7.88		33.4(1.0)	15.2(1.3)	30.6(1.1)	5.5(1.5)	15.4(1.2)

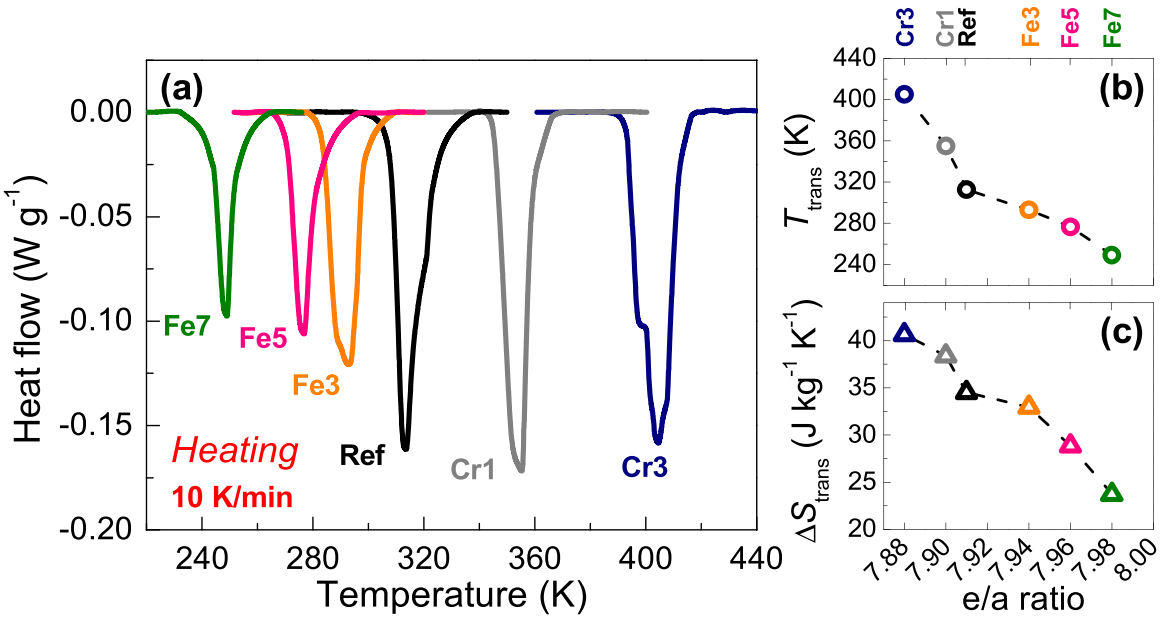

Fig. 3. (a) DSC curves for the studied series, (b) obtained martensitic to austenitic phase transformation temperatures and (c) entropy change of the transformation. Each of the compositions have the same color code for all panels.

the strong overlap of both martensitic and Curie transitions, which leads to a martensitic transformation between two paramagnetic phases [29]. Therefore, Cr3 sample is discarded from further magnetic analysis due to its low magnetic response. The magnetization values obtained for the alloy series at a field of 9 T are displayed in Fig. 4**c,** where the high magnetization values correspond to the austenitic phase and low magnetization values correspond to the martensitic phase.

Isothermal entropy change is plotted as a function of temperature for the different field changes up to 9 T in Fig. 5**a**. It is worth mentioning that after all the measurements, the integrity of the pieces remains unaltered, making a significant difference when compared with other first-order MC materials [42,43]. The trend of ΔS_{iso} with e/a ratio is not comparable with the one observed previously for the transformation entropy change. This is because the values of ΔS_{iso} for the different samples depend on the chosen magnetic field change. For fields as high as 9 T, maximum values are found for the Fe3 sample (which slightly improve the values of the reference sample). For larger Fe and Cr contents, the values are lower (specially for the Cr case). The arrows in Fig. 5**a** indicate the total entropy change due to the martensitic transformation obtained by DSC, in order to compare how relevant the decrease of ΔS_{iso} is with respect to the saturation values of the entropy change when the transformation is driven by the field. It is observed that as the e/a ratio increases, the ΔS_{iso} values are closer to ΔS_{trans}, reaching the same value for the Fe7 sample. This indicates that Fe doping helps to decrease the field needed to complete the transformation, reaching saturation for a magnetic field change of 7 T. However, as ΔS_{trans} decreases with increasing e/a ratio, maximum ΔS_{iso} values for 9 T are smaller for Fe7 in comparison to the reference sample. Nevertheless, for the technologically relevant field range of 2 T, we find that ΔS_{iso} values increase with increasing e/a ratio. Comparing to the reference sample, there is an increase of 20% for Fe7. This is a significant improvement caused by the replacement of Mn by Fe. Fig. 5**b** shows the evolution of the transition temperature with the magnetic field for the studied series, together with a comparison with the values predicted by the Clausius-Clapeyron relation $\frac{dT_{trans}}{dH} = -\frac{\Delta M}{\Delta S_{trans}}$ [14]. A good agreement between the experimental results and the Clausius-Clapeyron relation is obtained, reinforcing the analysis performed. Notably, there is a significant increase of the field evolution of the transformation with increasing e/a ratio, having a 100% increase for Fe7 sample with respect to the reference. In addition, this feature leads to broader magnetocaloric peaks for a given magnetic field change. For example, the width of the ΔS_{iso} for Fe7 increases with respect to the reference from 20 K to 24 K for 2 T. This also proves the

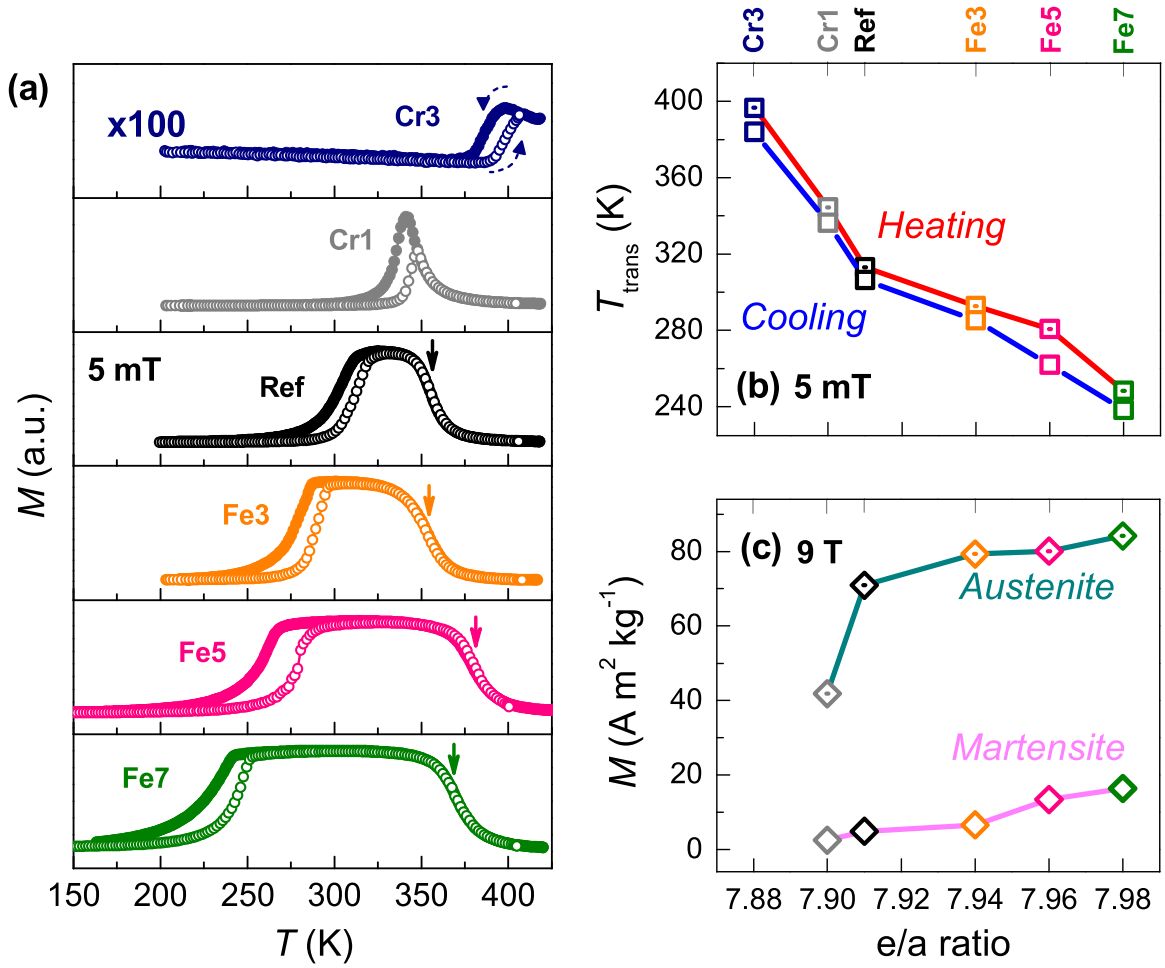

Fig. 4. (a) Temperature dependence of magnetization for low fields for the studied series where arrows illustrate the value of T_c. (b) Martensitic transition temperatures and (c) austenite and martensite magnetization around the transformation temperature for 9 T.

enhanced MC applicability of the system due to Mn substitution by Fe. It is worth noting that Cr increases the entropy change due to transformation (Fig. 3**c**), which could be beneficial for baro-/elasto-caloric applications where magnetization does not play a significant role.

To compare the MC response of this alloy series with literature data, Fig. 5**c** collects different *TEC* (5) values for 2 T for similar Ni-Co-Mn-Ti alloys [24,25,44], including other Fe-doped alloys [27,28,45–47]. The figure indicates that the synthetized series has an enhanced response in comparison to other reported alloys. Literature survey suggests that, on the one hand, when Fe substitutes Ni, it plays a similar role as Co [27]. This Fe/Ni substitution strategy causes a significant decrease of the MC response [27]. Fe and Co can also be added together substituting Ni. Through this strategy, the MC response at 2 T slightly decreases as the (FeCo) content increases from 16 to 20 at% [28]. On the other hand, Fe can be used for substituting Mn (as in the present work). While a recent study in which Fe/Mn substitution is performed did not show a clear trend for the magnetocaloric effect [47], our work shows that Fe/Mn substitution clearly decreases the required field for saturating the transformation, which compensates the decrease in the transformation entropy change. The other doping direction of Mn substitution by Cr followed in this work produces a larger overlap between the Curie and martensitic transitions, decreasing the magnetic moment and therefore the total magnetocaloric response.

Fig. 6**a** shows the temperature dependence of exponent n for the studied series for a magnetic field change of 9 T. A clear overshoot above 2 can be observed at temperatures lower than those of the peak temperature, which is typical for inverse MC materials. This overshoot indicates the first-order character of the transformations. Interestingly, the magnitude of the overshoot is similar for all the compositions except for Cr1, the one with smaller magnetization difference among austenite and martensite. Moreover, the values of the exponent n at temperatures close to the transition temperature for 9 T gives information about the evolution of the transformation with the magnetic field. Negative values of exponent n are mainly observed for Fe7 sample, indicating that ΔS_{iso} values are decreasing with field. This occurs once the FOPT is completed, with the corresponding inverse ΔS_{iso} saturated, while the response of overlapping Curie transition of the austenitic phase (of opposite sign) is still increasing with field, as described in [30]. For lower e/a ratio samples, the exponent n values are much closer to zero or even positive after the overshoot, indicating that the inverse MC response is still far from being saturated. This agrees with the analysis of the ΔS_{iso} values with respect to the ΔS_{trans} obtained from DSC. The character of the transformation can also be studied from Arrott plots by applying the Banerjee's criterion: negative slopes in the H/M vs. M^2 plots correspond to first-order transitions while positive ones indicate second-order. Fig. 6**b** shows the Arrott plots for the alloy series at temperatures close to the martensitic transformation for each sample for

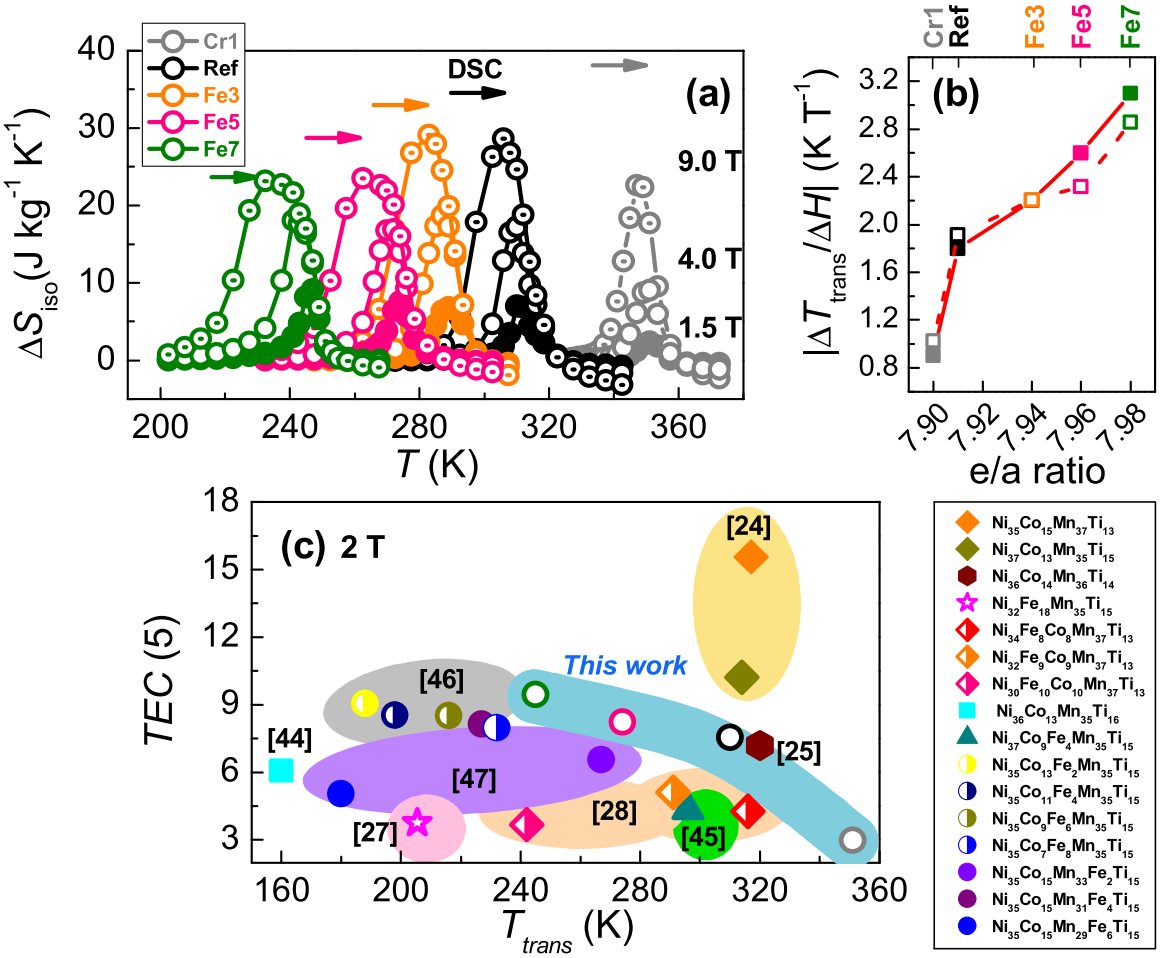

Fig. 5. (a) Temperature dependence of the heating isothermal entropy change. Arrows indicate the transition entropy change obtained from DSC. (b) Transition temperature shift with magnetic field (solid symbols) and predicted values by Clausius-Clapeyron relation (hollow symbols). (c) Comparison to other reported bulk Ni(Co)-Mn-Ti alloys (data interpolation for 2 T has been employed for [28]).

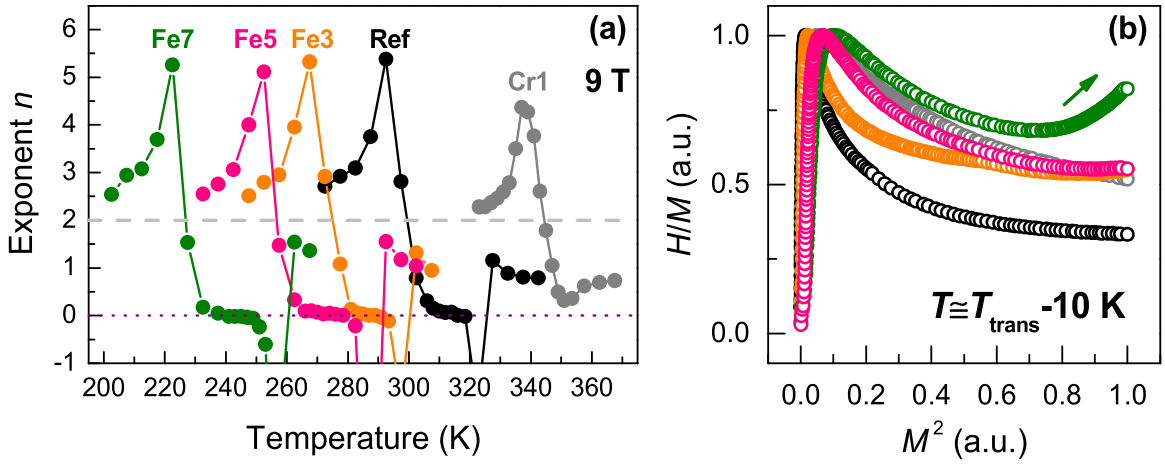

Fig. 6. (a) Temperature dependence of the exponent n and (b) Arrott plots for the studied series (except Cr3) for a temperature 10 K below the transition temperature.

applied fields up to 9 T. From the Arrott plots, it is evident that all the samples belong to the first-order category, in agreement with previous exponent *n* results. Furthermore, it can be observed that the transformation for Fe7 is completed for 9 T as positive slopes can be recovered at fields around 7 T as indicated with the arrow in Fig. 6**b**. This serves as further confirmation of previously presented analysis.

4. Conclusions

A series of all-d-metal Ni-Co-Mn(X)-Ti Heusler alloys been investigated employing X=Fe or Cr as dopants. On the one hand, Cr doping shifts the martensitic transition to higher temperatures while decreasing the Curie temperature of the austenitic phase and increases the entropy change due to the transition. The increasing overlap between martensitic and Curie transitions with Cr doping causes a significant deterioration of the MC response, although the transition entropy change is higher. On the other hand, Fe doping shifts the martensitic transition to lower temperatures while slightly increases the Curie temperature of the austenitic phase and decreases the entropy change during the transformation (from 35 J kg^{-1} K^{-1} for the reference down to 23 J kg^{-1} K^{-1} for Fe7 sample). However, it is shown that as Fe content increases, the saturation of the magnetocaloric effect is reached for lower fields due to an improved field evolution of the transition. These features for Fe doping lead to improved isothermal entropy changes for moderate magnetic field changes, showing an increment of 20% for the Fe7 sample with respect to the parent composition for 2 T. This work, on the one hand, evidences the importance of the overlapping between Curie and martensitic transformations for modulating the isothermal entropy change of a sample with even large transformation entropy change. On the other hand, lowering the magnetic field required for saturating the transformation also plays a significant role in the practical applicability of magnetocaloric materials. For these reasons, Mn substitution by Fe is a useful way for improving the magnetocaloric applicability of the Ni-Co-Mn-Ti system.

CRediT authorship contribution statement

A.N. Khan: Investigation, Methodology, Formal analysis, Writing – original draft. **L.M. Moreno-Ramírez**: Conceptualization, Investigation, Methodology, Formal analysis, Supervision, Writing – review & editing. **Á. Díaz-García**: Investigation, Methodology, Formal analysis, Writing – review & editing. **J.Y. Law**: Investigation, Methodology, Formal analysis, Writing – review & editing. **V. Franco**: Conceptualization, Methodology, Formal analysis, Writing – review & editing, Supervision, Funding acquisition.

Data availability

Data will be made available on request.

Declaration of Competing Interest

The authors declare that they have no known competing financial interests or personal relationships that could have appeared to influence the work reported in this paper.

Acknowledgements

Work supported by Grant PID2019-105720RB-I00 funded by MCIN/AEI/10.13039/501100011033, Consejería de Economía, Conocimiento, Empresas y Universidad de la Junta de Andalucía (grant P18-RT-746), US Air Force Office of Scientific Research (FA8655-21-1-7044) and Sevilla University under VI PPIT-US program. ANK acknowledges a FPI fellowship from the Spanish MCIN/AEI. LMMR acknowledges a postdoctoral fellowship from Junta de Andalucía and European Social Fund (ESF).

References

[1] V.K. Pecharsky, K.A. Gschneidner Jr, Magnetocaloric effect and magnetic refrigeration, J. Magn. Magn. Mater. 200 (1999) 44–56, https://doi.org/10.1016/S0304-8853(99)00397-2
[2] V. Franco, J.S. Blázquez, J.J. Ipus, J.Y. Law, L.M. Moreno-Ramírez, A. Conde, Magnetocaloric effect: from materials research to refrigeration devices, Prog. Mater. Sci. 93 (2018) 112–232, https://doi.org/10.1016/J.PMATSCI.2017.10.005
[3] O. Gutfleisch, M.A. Willard, E. Brück, C.H. Chen, S.G. Sankar, J.P. Liu, Magnetic materials and devices for the 21st century: stronger, lighter, and more energy efficient, Adv. Mater. 23 (2011) 821–842, https://doi.org/10.1002/adma.201002180
[4] A. Kitanovski, Energy applications of magnetocaloric materials, Adv. Energy Mater. 10 (2020) 1903741, https://doi.org/10.1002/aenm.201903741
[5] H. Zhang, R. Gimaev, B. Kovalev, K. Kamilov, V. Zverev, A. Tishin, Review on the materials and devices for magnetic refrigeration in the temperature range of nitrogen and hydrogen liquefaction, Phys. B Condens. Matter 558 (2019) 65–73, https://doi.org/10.1016/J.PHYSB.2019.01.035
[6] V. Franco, Magnetocaloric characterization of materials, Magnetic Measurement Techniques for Materials Characterization, Springer International Publishing, Cham, 2021, pp. 697–726, https://doi.org/10.1007/978-3-030-70443-8_23
[7] V.K. Pecharsky, K.A. Gschneidner Jr, Giant magnetocaloric effect in Gd5(Si2Ge2), Phys. Rev. Lett. 78 (1997) 4494–4497, https://doi.org/10.1103/PhysRevLett.78.4494
[8] T. Gottschall, K.P. Skokov, M. Fries, A. Taubel, I. Radulov, F. Scheibel, D. Benke, S. Riegg, O. Gutfleisch, Making a cool choice: the materials library of magnetic refrigeration, Adv. Energy Mater. 9 (2019) 1901322, https://doi.org/10.1002/aenm.201901322
[9] A. Fujita, S. Fujieda, Y. Hasegawa, K. Fukamichi, Itinerant-electron metamagnetic transition and large magnetocaloric effects in La(FexSi1-x)13 compounds and their hydrides, Phys. Rev. B 67 (2003) 104416, https://doi.org/10.1103/PhysRevB.67.104416
[10] J. Liu, J.D. Moore, K.P. Skokov, M. Krautz, K. Löwe, A. Barcza, M. Katter, O. Gutfleisch, Exploring La(Fe,Si)13-based magnetic refrigerants towards application, Scr. Mater. 67 (2012) 584–589, https://doi.org/10.1016/J.SCRIPTAMAT.2012.05.039
[11] O. Tegus, E. Brück, K.H.J. Buschow, F.R. de Boer, Transition-metal-based magnetic refrigerants for room-temperature applications, Nature 415 (2002) 150–152, https://doi.org/10.1038/415150a
[12] A. Planes, L. Mañosa, M. Acet, Magnetocaloric effect and its relation to shape-memory properties in ferromagnetic Heusler alloys, J. Phys. Condens. Matter 21 (2009) 233201, https://doi.org/10.1088/0953-8984/21/23/233201
[13] J. Liu, T. Gottschall, K.P. Skokov, J.D. Moore, O. Gutfleisch, Giant magnetocaloric effect driven by structural transitions, Nat. Mater. 11 (2012) 620–626, https://doi.org/10.1038/nmat3334
[14] C. Felser, A. Hirohata, Heusler Alloys: Properties, Growth, Applications, Springer International Publishing, Cham, 2016, https://doi.org/10.1007/978-3-319-21449-8
[15] X. Moya, L. Mañosa, A. Planes, T. Krenke, M. Acet, E.F. Wassermann, Martensitic transition and magnetic properties in Ni–Mn–X alloys, Mater. Sci. Eng. A 438–440 (2006) 911–915, https://doi.org/10.1016/J.MSEA.2006.02.053
[16] A. Planes, L. Mañosa, M. Acet, Magnetocaloric effect and its relation to shape-memory properties in ferromagnetic Heusler alloys, J. Phys. Condens. Matter 21 (2009) 233201, https://doi.org/10.1088/0953-8984/21/23/233201
[17] D. Comtesse, M. Gruner, V. Sokolovskiy, V. Buchelnikov, A. Grünebohm, R. Arróyave, N. Singh, T. Gottschall, O. Gutfleisch, V. Chernenko, F. Albertini, S. Fähler, P. Entel, First-principles calculation of the instability leading to giant inverse magnetocaloric efects, Phys. Rev. B 89 (2014) 184403, https://doi.org/10.1103/PhysRevB.89.184403
[18] T. Bachagha, J. Zhang, M. Khitouni, J. Suñol, NiMn-based Heusler magnetic shape memory alloys: a review, Int. J. Adv. Manuf. Technol. 103 (2019) 2761–2772, https://doi.org/10.1007/s00170-019-03534-3
[19] H. le Yan, H.X. Liu, Y. Zhao, N. Jia, J. Bai, B. Yang, Z. Li, Y. Zhang, C. Esling, X. Zhao, L. Zuo, Impact of B alloying on ductility and phase transition in the Ni–Mn-based magnetic shape memory alloys: insights from first-principles calculation, J. Mater. Sci. Technol. 74 (2021) 27–34, https://doi.org/10.1016/J.JMST.2020.10.010
[20] Z.Y. Wei, E.K. Liu, Y. Li, X.L. Han, Z.W. Du, H.Z. Luo, G.D. Liu, X.K. Xi, H.W. Zhang, W.H. Wang, G.H. Wu, Magnetostructural martensitic transformations with large volume changes and magneto-strains in all-d-metal Heusler alloys, Appl. Phys. Lett. 109 (2016) 071904, https://doi.org/10.1063/1.4961382
[21] V.G. de Paula, M.S. Reis, All-d-Metal Full Heusler alloys: a novel class of functional materials, Chem. Mater. 33 (2021) 5483–5495, https://doi.org/10.1021/acs.chemmater.1c01012
[22] Z.Y. Wei, E.K. Liu, J.H. Chen, Y. Li, G.D. Liu, H.Z. Luo, X.K. Xi, H.W. Zhang, W.H. Wang, G.H. Wu, Realization of multifunctional shape-memory ferromagnets in all-d-metal Heusler phases, Appl. Phys. Lett. 107 (2015) 022406, https://doi.org/10.1063/1.4927058
[23] H. Neves Bez, A.K. Pathak, A. Biswas, N. Zarkevich, V. Balema, Y. Mudryk, D.D. Johnson, V.K. Pecharsky, Giant enhancement of the magnetocaloric response in Ni–Co–Mn–Ti by rapid solidification, Acta Mater. 173 (2019) 225–230, https://doi.org/10.1016/J.ACTAMAT.2019.05.004

[24] A. Taubel, B. Beckmann, L. Pfeuffer, N. Fortunato, F. Scheibel, S. Ener, T. Gottschall, K.P. Skokov, H. Zhang, O. Gutfleisch, Tailoring magnetocaloric effect in all-d-metal Ni-Co-Mn-Ti Heusler alloys: a combined experimental and theoretical study, Acta Mater. 201 (2020) 425–434, https://doi.org/10.1016/J.ACTAMAT.2020.10.013
[25] Z.-Q. Guan, J. Bai, Y. Zhang, J.-L. Gu, X.-J. Jiang, X.-Z. Liang, R.-K. Huang, Y.-D. Zhang, C. Esling, X. Zhao, L. Zuo, Revealing essence of magnetostructural coupling of Ni-Co-Mn-Ti alloys by first-principles calculations and experimental verification, Rare Met. 41 (2022) 1933–1947, https://doi.org/10.1007/s12598-021-01947-2
[26] A. Díaz-García, L.M. Moreno-Ramírez, J.Y. Law, F. Albertini, S. Frabbrici, V. Franco, Characterization of thermal hysteresis in magnetocaloric NiMnIn Heusler alloys by Temperature First Order Reversal Curves (TFORC), J. Alloy. Compd. 867 (2021) 159184, https://doi.org/10.1016/J.JALLCOM.2021.159184
[27] Q. Zeng, J. Shen, H. Zhang, J. Chen, B. Ding, X. Xi, E. Liu, W. Wang, G. Wu, Electronic behaviors during martensitic transformations in all-d-metal Heusler alloys, J. Phys. Condens. Matter 31 (2019) 425401, https://doi.org/10.1088/1361-648X/ab2bd8
[28] S. Samanta, S. Ghosh, S. Chatterjee, K. Mandal, Large magnetocaloric effect and magnetoresistance in Fe-Co doped Ni50-x(FeCo)xMn37Ti13 all-d-metal Heusler alloys, J. Alloy. Compd. 910 (2022) 164929, https://doi.org/10.1016/J.JALLCOM.2022.164929
[29] J.Y. Law, Á. Díaz-García, L.M. Moreno-Ramírez, V. Franco, A. Conde, A.K. Giri, How concurrent thermomagnetic transitions can affect magnetocaloric effect: the Ni49+xMn36-xIn15 Heusler alloy case, Acta Mater. 166 (2019) 459–465, https://doi.org/10.1016/J.ACTAMAT.2019.01.007
[30] Á. Díaz-García, J.Y. Law, L.M. Moreno-Ramírez, A.K. Giri, V. Franco, Deconvolution of overlapping first and second order phase transitions in a NiMnIn Heusler alloy using the scaling laws of the magnetocaloric effect, J. Alloy. Compd. 871 (2021) 159621, https://doi.org/10.1016/J.JALLCOM.2021.159621
[31] J.S. Amaral, V.S. Amaral, On estimating the magnetocaloric effect from magnetization measurements, J. Magn. Magn. Mater. 322 (2010) 1552–1557, https://doi.org/10.1016/j.jmmm.2009.06.013
[32] L. Tocado, E. Palacios, R. Burriel, Entropy determinations and magnetocaloric parameters in systems with first-order transitions: study of MnAs, J. Appl. Phys. 105 (2009) 093918, https://doi.org/10.1063/1.3093880
[33] L. Caron, Z.Q. Ou, T.T. Nguyen, D.T. Cam Thanh, O. Tegus, E. Brück, On the determination of the magnetic entropy change in materials with first-order transitions, J. Magn. Magn. Mater. 321 (2009) 3559–3566, https://doi.org/10.1016/J.JMMM.2009.06.086
[34] V. Franco, A. Conde, Scaling laws for the magnetocaloric effect in second order phase transitions: from physics to applications for the characterization of materials, Int. J. Refrig. 33 (2010) 465–473, https://doi.org/10.1016/j.ijrefrig.2009.12.019
[35] L.D. Griffith, Y. Mudryk, J. Slaughter, V.K. Pecharsky, Material-based figure of merit for caloric materials, J. Appl. Phys. 123 (2018) 034902, https://doi.org/10.1063/1.5004173
[36] J.Y. Law, L.M. Moreno-Ramírez, Á. Díaz-García, A. Martín-Cid, S. Kobayashi, S. Kawaguchi, T. Nakamura, V. Franco, MnFeNiGeSi high-entropy alloy with large magnetocaloric effect, J. Alloy. Compd. 855 (2021) 157424, https://doi.org/10.1016/J.JALLCOM.2020.157424
[37] J.Y. Law, Á. Díaz-García, L.M. Moreno-Ramírez, V. Franco, Increased magnetocaloric response of FeMnNiGeSi high-entropy alloys, Acta Mater. 212 (2021) 116931, https://doi.org/10.1016/J.ACTAMAT.2021.116931
[38] H. le Yan, L. da Wang, H.X. Liu, X.M. Huang, N. Jia, Z. bin Li, B. Yang, Y.D. Zhang, C. Esling, X. Zhao, L. Zuo, Giant elastocaloric effect and exceptional mechanical properties in an all-d-metal Ni–Mn–Ti alloy: experimental and ab-initio studies, Mater. Des. 184 (2019) 108180, https://doi.org/10.1016/J.MATDES.2019.108180
[39] S. Samanta, S. Chatterjee, S. Ghosh, K. Mandal, Large reversible magnetocaloric effect and magnetoresistance by improving crystallographic compatibility condition in Ni(Co)-Mn-Ti all-d-metal Heusler alloys, Phys. Rev. Mater. 6 (2022) 94411, https://doi.org/10.1103/PhysRevMaterials.6.094411
[40] S. Singh, P. Kushwaha, F. Scheibel, H.-P. Liermann, S.R. Barman, M. Acet, C. Felser, D. Pandey, Residual stress induced stabilization of martensite phase and its effect on the magnetostructural transition in Mn-rich Ni-Mn-In/Ga magnetic shape-memory alloys, Phys. Rev. B 92 (2015) 20105, https://doi.org/10.1103/PhysRevB.92.020105
[41] A.M. Tishin, Y.I. Spichkin, The magnetocaloric effect and its applications, Mater. Today 6 (2003) 51, https://doi.org/10.1016/S1369-7021(03)01134-9
[42] X. Zhang, H. Zhang, M. Qian, L. Geng, Enhanced magnetocaloric effect in Ni-Mn-Sn-Co alloys with two successive magnetostructural transformations, Sci. Rep. 8 (2018) 8235, https://doi.org/10.1038/s41598-018-26564-5
[43] N.M. Bruno, S. Yuce, On the instability of the giant direct magnetocaloric effect in CoMn0.915Fe0.085Ge at% metamagnetic compounds, Sci. Rep. 10 (2020) 14211, https://doi.org/10.1038/s41598-020-71149-w
[44] Z. Guan, J. Bai, Y. Zhang, J. Gu, X. Liang, Y. Zhang, C. Esling, X. Zhao, L. Zuo, Simultaneously realized large low-temperature magnetocaloric effect and good mechanical properties in Ni36Co13Mn35Ti16 alloy, J. Appl. Phys. 131 (2022) 165107, https://doi.org/10.1063/5.0088692
[45] S. Liu, H. Xuan, T. Cao, L. Wang, Z. Xie, X. Liang, H. Li, L. Feng, F. Chen, P. Han, Magnetocaloric and elastocaloric effects in All-d-Metal Ni37Co9Fe4Mn35Ti15 magnetic shape memory alloy, Phys. Status Solidi (a) 216 (2019) 1900563, https://doi.org/10.1002/pssa.201900563
[46] Y. Li, S. Huang, W. Wang, E. Liu, L. Li, Ferromagnetic martensitic transformation and large magnetocaloric effect in Ni35Co15−xFexMn35Ti15 (x = 2, 4, 6, 8) alloys, J. Appl. Phys. 127 (2020) 233907, https://doi.org/10.1063/5.0001403
[47] Y. Li, L. Qin, S. Huang, L. Li, Enhanced magnetocaloric performances and tunable martensitic transformation in Ni35Co15Mn35−xFexTi15 all-d-metal Heusler alloys by chemical and physical pressures, Sci. China Mater. 65 (2022) 486–493, https://doi.org/10.1007/s40843-021-1747-3